ELSEVIER

Biophysical Chemistry 101–102 (2002) 577–591

Biophysical Chemistry

www.elsevier.com/locate/bpc

Interaction of bombolitin II with a membrane-mimetic environment: an NMR and molecular dynamics simulation approach☆

Luca Monticelli, Davide Pedini, Elisabetta Schievano, Stefano Mammi, Evaristo Peggion*

Department of Organic Chemistry, University of Padova, Biopolymer Research Center, C.N.R., 35131 Padua, Italy

Abstract

Bombolitins are five natural heptadecapeptides originally isolated from the venom of a bumblebee. They induce lysis of erythrocytes and liposomes and increase the activity of phospholipase A_2 (PLA_2), that plays an important role in the early steps of the inflammatory process. It has been proposed that PLA_2 activation depends on the alteration of the physical state of the membrane. Bombolitin II folds into an α-helix in a membrane mimicking environment constituted by sodium dodecyl sulfate micelles (Macromol. Chem. Phys., 196 (1995) 2827). In the present work, the topological orientation of the peptide relative to the micelle was determined, using three spin probes localized in different positions of the water/micelle system. The reduction in intensity of the ^{1}H NMR signals clearly demonstrated that the peptide is located on the surface of the micelle, with its helical axis parallel to the interface. Only a small portion of the helix is exposed to the aqueous environment. Results from NMR experiments were confirmed by molecular dynamics simulations, performed using a two-phase water/decane simulation cell. The timescale for the reorientation of the peptide was between 120 and 450 ps, depending on the starting position of the peptide.

Keywords: Bombolitin; Micelle; Sodium dodecyl sulfate; Spin probe; Computer simulation; Molecular dynamics; NMR

1. Introduction

Bombolitins are five natural heptadecapeptides originally isolated from the venom of a bumblebee, the *Megabombus pennsylvanicus*. They share high homology in the amino acid sequence and similarities in the conformational properties and biological activity. They induce lysis of erythrocytes and liposomes [1], and enhance the activity of phospholipase A_2 (PLA_2), responsible for the release of arachidonic acid through the hydrolysis of membrane phospholipids in one of the early steps of the inflammatory process.

Bombolitins are amphipathic peptides that adopt α-helical conformations in the presence of an amphipathic environment such as aqueous solutions containing sodium dodecyl sulfate (SDS) [2,3]. A simple method was published in 1982 [4]

☆ Dedicated to John A. Schellman on the occasion of his 80th birthday.

*Corresponding author. Tel.: +39-49-827-5262; fax: +39-49-827-5239.

E-mail address: evaristo.peggion@unipd.it (E. Peggion).

0301-4622/02/$ - see front matter
PII: S0301-4622(02)00174-6

to predict the propensity of a helical peptide to lie on the surface of a membrane, to enter its hydrophobic interior or to be part of a globular protein. The method is based on the helical hydrophobic moment and the average hydrophobicity of the peptide, and amphipathic helices are divided into seven classes according to these parameters and to other physico-chemical properties [5]. Amphipathic peptides with lytic activity belong to class L, and they are characterized by a high hydrophobic moment, the abundance of basic (lysine) residues and a narrow hydrophilic helical surface ($<100°$); according to the Eisenberg diagram [4], they are predicted to lie on membrane surfaces.

Previous studies on enantiomeric and on retro sequences of bombolitin I and bombolitin III have shown that the activation of PLA_2 does not depend on specific enzyme–peptide interactions; retro sequences and D-peptides have the same biological activity as native bombolitins, indeed. Therefore, it has been proposed that PLA_2 activation depends on modifications of the physical state of the membrane [3,6]. For this reason, investigations of the interaction between the peptide and the lipid can provide an important contribution to understand the origin of the inflammatory process.

Bombolitin II adopts an α-helical structure in a membrane-mimicking environment, provided by SDS micelles [3]. The main goal of the present research is to determine the topological orientation of the peptide relative to the micelle. Several techniques are available to get an insight on this problem; we chose to exploit the change of the relaxation properties of ^1H nuclei in the peptide caused by dipolar interaction with the unpaired electron of spin probes. Rather than measuring relaxation rates, we utilized the reduction in intensity of appropriate cross-peaks in TOCSY spectra. We utilized three different spin probes, localized in different positions of the water/micelle environment. The experimental results were then compared to a molecular modeling study, in order to test the possibility of predicting the orientation of amphipathic helical peptides in a micellar environment using molecular dynamics (MD) simulations.

2. Methods

Bombolitin II was synthesized as previously described [3]. The NMR experiments were performed on a Bruker AVANCE DMX600 spectrometer and data were processed on an SGI Indy workstation (R5000), using the XWINNMR software. Data were collected on 3 mM bombolitin II samples in water (9:1 $H_2O/^2H_2O$) at pH 4.5 (uncorrected), in the presence of 300 mM SDS-d_{25} (CIL). Under these conditions, SDS forms stable micelles with approximately 90 SDS molecules/micelle [7]. All spectra were recorded at 313 K.

One-dimensional ^1H spectra were acquired with presaturation to achieve water suppression, collecting 64 transients and 32K data points.

Two-dimensional homonuclear ^1H spectra were recorded in pure absorption mode according to the TPPI method with 300 experiments of 4K data points. Prior to Fourier transformation, the time domain data points were multiplied by phase-shifted squared sine or Gaussian window functions in both dimension, and zero-filled to $1K\times4K$ real points. The homonuclear Hartmann-Hahn spectra were performed in the version proposed by Griesinger et al. [8] (clean-TOCSY). The MLEV-17 spin lock sequence, preceded by a 2.5 ms trim pulse, was applied for a total mixing time of 51–52 ms. Suppression of the water signal was achieved with the WATERGATE sequence [9] before FID acquisition.

The 5-doxyl-stearic acid (5-DSA) and 16-doxyl-stearic acid (16-DSA) were added as solid powder to two equivalent solutions containing the peptide and the SDS to obtain a final concentration of 3 mM for each spin probe. The same procedure was followed to introduce different aliquots of 2,2,6,6-tetramethylpiperidine-1-oxyl-4-amino-4-carboxylic acid (Toac) in order to obtain concentrations ranging from 2 to 10 mM. No precipitation occurred upon addition of any of the spin probes. Clean-TOCSY experiments were recorded under identical conditions before and after the addition of the spin probe. The error on the intensities of the cross-peaks were estimated from two TOCSY spectra recorded and processed in the same conditions and is lower than 5%.

Previously derived interproton distances [3] were used as upper limits in the distance geometry (DG) and distance-driven MD, following standard procedures. The non-redundant distances were 123. Volume constraints were used to avoid the forma-

tion of left-handed helices. This procedure yielded 58 structures fulfilling the holonomic and experimental constraints (with no NOE violations >0.3 Å). All DG and distance-driven MD calculations were carried out using a non-commercial program based on the Havel algorithm (courtesy of Prof. Dale F. Mierke, Brown University, Providence, RI, USA), on an SGI O2 (R5000) workstation.

All the MD simulations were carried out using explicit solvent, and decane was chosen to mimic the membrane environment. Clearly, decane lacks a number of important features of real membranes, including polar headgroups and the associated charge distribution, the structured long lipid tails and the non-uniform density and pressure profiles of real lipid bilayers or micelles. The main advantages of simulations with decane as a membrane mimetic are (i) a decent representation of water and of the hydrophobic membrane interior and (ii) the computational simplicity; moreover, (iii) the dynamics of decane are much faster than that of lipids, and the motions of peptides in hydrocarbons are faster than in lipids as well.

The biphasic system consisted of approximately 140 decane molecules and 1400 water molecules; the size of the simulation box was 4.4 nm in the x and y dimensions, and approximately 5.4 nm in the z dimension; water and decane atoms were removed within van der Waals distance from the peptide. These systems were energy minimized and used as starting structures for MD simulations.

For all MD simulations, the GROMOS87 force field with all hydrogens, as implemented in GROMACS (version 2.0, University of Groningen, the Netherlands [10]) was used. The water model used was SPC [11]. The CH_2 and CH_3 groups of decane were treated as united atoms, the Ryckaert-Bellemans potential was applied and a minimum distance of 0.23 nm between water and decane molecules was allowed.

Water, peptide and decane were coupled separately to a temperature bath at 300 K with $t_T=0.1$ ps [12]. The surface area of the system was fixed, and the pressure in the z direction was kept at 1 bar using weak pressure coupling with $t_p=1.0$ ps.

As the peptide contains four basic residues (Lys^2, Lys^9, Lys^{12}, His^{16}) and an acidic one (Asp^5), several possible charge states can be chosen for their side chains; MD simulations were carried out both with neutral peptides and positively charged peptides. In the case of neutral peptides, Lys^9 and Asp^5 side chains were ionized, while in the case of positively charged systems we chose the most likely state at pH 7, with all lysines and the aspartic acid charged, and the histidine neutral. A group-based twin-range cutoff of 0.9–1.5 nm, without shift or switch function, was used for both Coulomb and Lennard–Jones interactions. As reported in the literature, alternative methods like reaction field corrections or Ewald summation are probably less appropriate for non-homogeneous systems consisting of areas with low dielectric

Table 1
Overview of the molecular dynamics simulations featured in this work

Simulation number	Simulation length (ns)	Time step (fs)	NOE restraints[a]	Charge[b]	Angle between the helical axis and the z-axis (°)
1	1	2	+	N	90
2	1	2	+	C	90
3	10	6	−	N	90
4	10	6	+	N	90
5	1	2	+	N	90[c]
6	1	6	+	N	90[c]
7	10	6	−	N	90[c]
8	1	2	+	N	30
9	1	2	+	N	35
10	10	6	+	N	5

[a] +, used; −, unused.
[b] N, neutral; C, charged.
[c] 180° rotation about the helical axis.

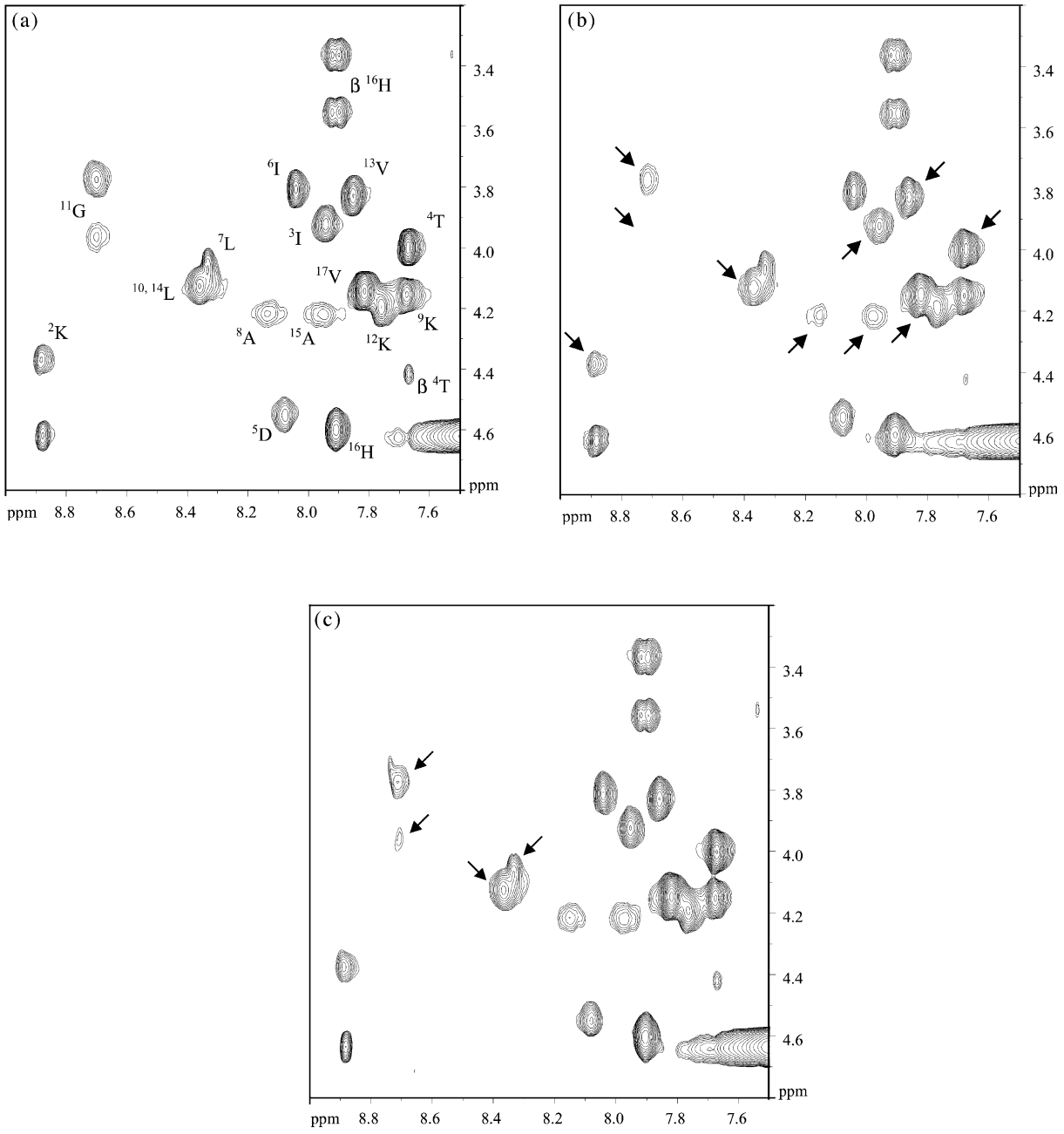

Fig. 1. Fingerprint region of the TOCSY spectrum of bombolitin II (3 mM in 300 mM SDS, D_2O/H_2O 1/9) in the (a) absence of spin probe (b) presence of 3 mM 5-DSA and (c) presence of 3 mM 16-DSA. Arrows indicate the signals that undergo remarkable reduction in intensity.

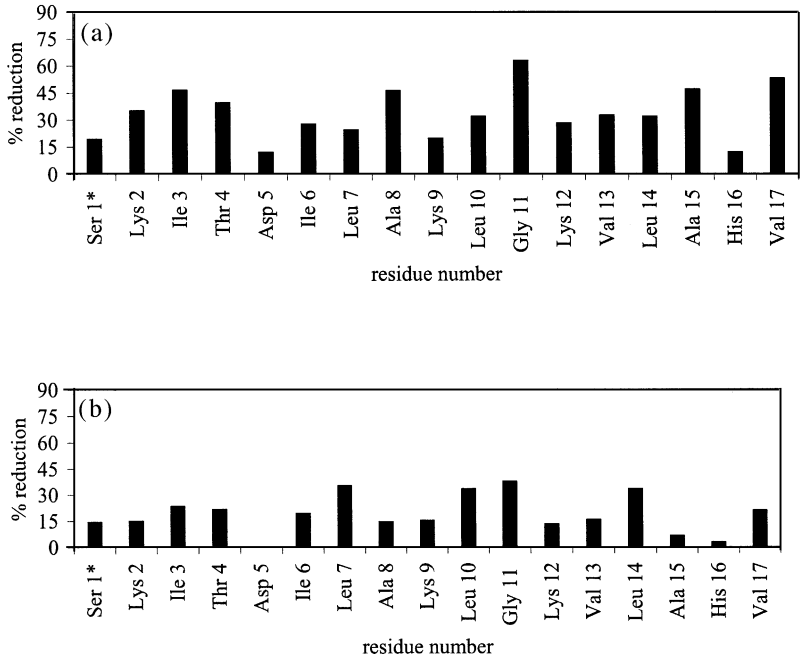

Fig. 2. Reduction of the intensity of the HN-Hα cross-peaks in the TOCSY spectrum upon addition (a) of 3 mM 5-DSA or (b) 3 mM 16-DSA. * Reduction of the intensity measured on the Hβ–Hβ peak.

constant, although detailed knowledge of the effect of different electrostatic approximation in membrane systems is currently not available [13].

A total of 10 MD simulations were performed with different timestep, total simulation time, starting orientation of the peptide and charge state; each of the 1 ns simulations (Table 1) was repeated twice, changing the seed number for the generation of starting velocities.

The timestep was 6 fs in simulations 3, 4, 6, 7 and 10 (Table 1); the neighbor list was updated every 3 timesteps. In all the other simulations the timestep was 2 fs, and the neighbor list was updated every 10 timesteps. In the former case, hydrogen atoms with an increased mass of 4 atomic mass units were used; hydrogens and the aromatic side chains were treated according to a published procedure [14], in order to remove degrees of freedom from the system. Briefly, forces on all hydrogens are calculated and not used to update the positions of the hydrogens but redistributed over neighboring heavy atoms; the positions of the hydrogens are recalculated at each step assuming an ideal geometry. This effectively removes degrees of freedom involving the hydrogen atoms, while still generating correct forces and

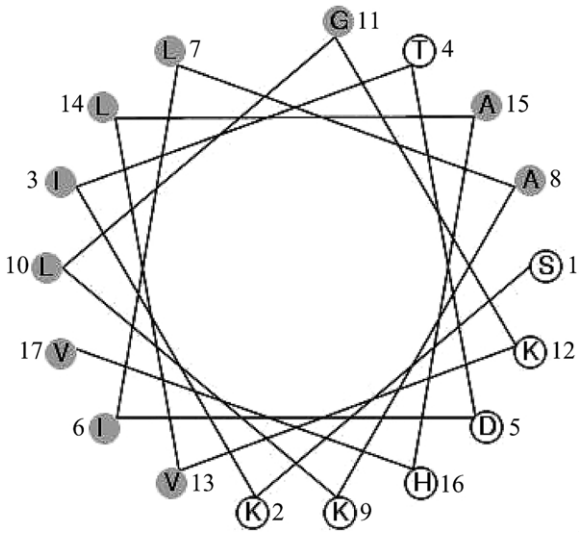

Fig. 3. Helical wheel representation of bombolitin II.

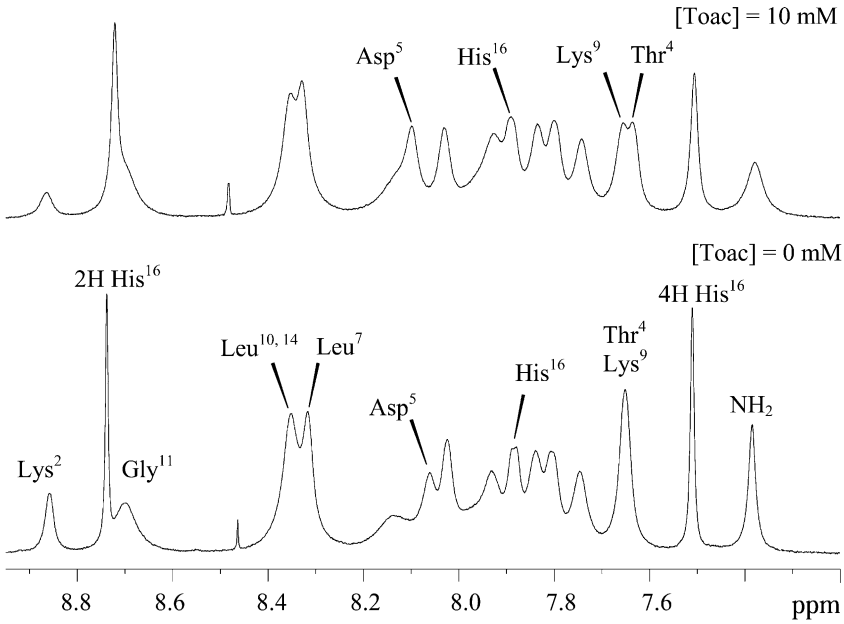

Fig. 4. Amide proton region of the 1D spectrum of bombolitin II (3 mM in 300 mM SDS, D_2O/H_2O 1/9) in the absence of spin probe (bottom) presence of 10 mM Toac (top).

pressure for the system as a whole. A similar method was also used for the calculation of the positions of the carbons in the aromatic rings, in order to remove degrees of freedom due to the loss of planarity. Bond lengths were constrained with the LINCS algorithm [15].

Before running the MD simulations, the system was energy minimized and the solvent was equil-

Table 2
Position of the interface and of bombolitin II in the simulation cell, secondary structure and reorientation time for the peptide during the MD simulations

Simulation number	Average z coordinate of the interface (nm)[a]	Average coordinate of the center of mass (nm)[a]	Residues in α-helical conformation[b]	Time required for reorientation (ps)
1	2.71	2.82	2–15	0
2	2.71	2.77	2–14	0
3	2.60 (2.62[c])	2.60 (2.56[c])	2–14	0
4	2.43 (2.43[c])	2.43 (2.43[c])	2–15	0
5	2.40	2.48	2–15	120
6	2.50	2.61	2–15	250
7	2.46 (2.47[c])	2.56 (2.45[c])	2–14	180
8	2.77	2.85	2–14	150
9	2.51	2.58	2–15	450
10	2.35	2.42	2–14	280

[a] Over the initial 1000 ps.
[b] For more than 80% of the simulation time.
[c] Over the final 1000 ps.

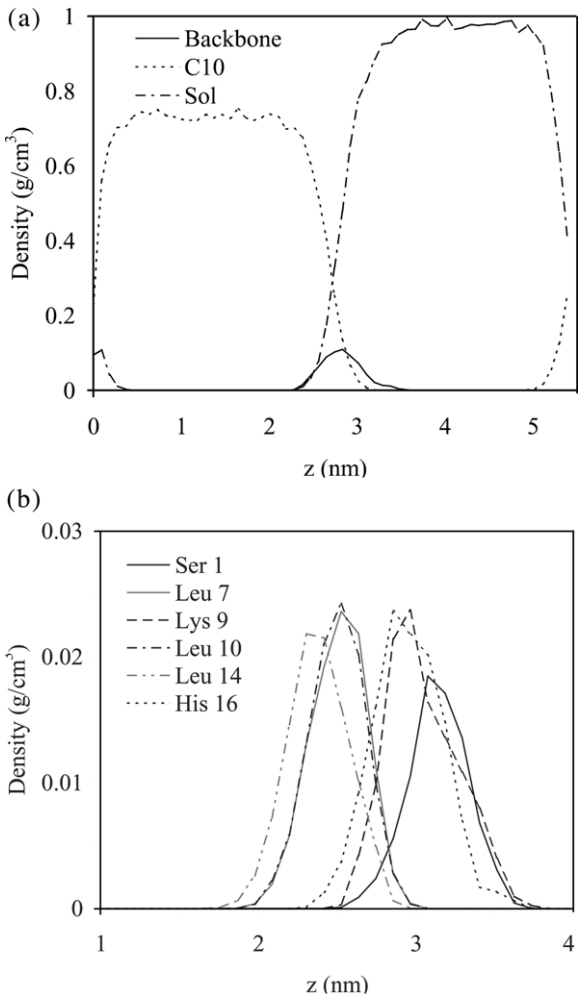

Fig. 5. (a) Density profile of the bombolitin II/decane/water system, averaged over 1 ns in simulation 1 (Table 1), with the peptide oriented according to the experimental results from the beginning of the MD; partial densities were calculated on the backbone atoms only. (b) Density profile of selected amino acids; partial densities were calculated including the side chain atoms, and averaged over 1 ns in simulation 1.

ibrated in a 50 ps MD run at 300 K, while the heavy atoms of the peptide were constrained to their initial position, with a force constant of 800 kJ mol^{-1} nm^{-2}. Subsequently, MD were performed at 300 K using the experimentally measured NOEs as distance restraints.

All MD simulations and their analyses were performed with programs in the GROMACS package [10]. For secondary structure analyses, definitions of DSSP [16] were used. Molecular graphics were made using INSIGHT II (Accelrys Inc.). Hydrogen bonds were defined geometrically: the hydrogen–donor–acceptor angle was less than 60° and the donor–acceptor distance less than 0.35 nm. Root mean square deviations (R.M.S.Ds) were calculated for backbone heavy atoms after fitting the Cα carbons to the initial model structure or, alternatively, for interatomic distances without any fitting.

3. Results and discussion

3.1. NMR and spin-probe experiments

To determine the position of bombolitin II in the SDS micelle, the spin probes 5-DSA, 16-DSA and Toac were used, that induce selective broadening of resonances from amino acids close to the paramagnetic probes.

As reported in the literature, when 5-DSA is dissolved in water in the presence of SDS micelles, the stearic acid chain is embedded in the micelle and the nitroxide group localizes close to the sulfate group [17]; the doxyl group broadens the resonances of SDS carbons 1–3 and those of the corresponding protons, close to the micelle surface. As for 16-DSA, the nitroxide group is found in a not very well defined region at the center of the micelle and broadens the resonances of SDS carbons in position 10–12 and those of the corresponding protons [17].

If we assume that the aggregation number of 300 mM SDS is 90 molecules [7], the micelle concentration should be approximately 3.3 mM. The concentration of DSA utilized was chosen to obtain a ratio [DSA]/[micelle] < 1. The probability of having two or more nitroxide molecules in the same micelle may be estimated using the Poisson distribution:

$$p(\geqslant 2) = 1 - [p(0) + p(1)] = 1 - (1 + p_{\max} N_A) e^{-p_{\max} N_A}$$

where $p_{\max} = [\mathrm{DSA}]/[\mathrm{SDS}]$ and N_A is the aggregation number of the micelle. With a DSA concentration of 3 mM, this probability is 0.22.

On the contrary, Toac is soluble in water and does not enter the micelle, making it useful to

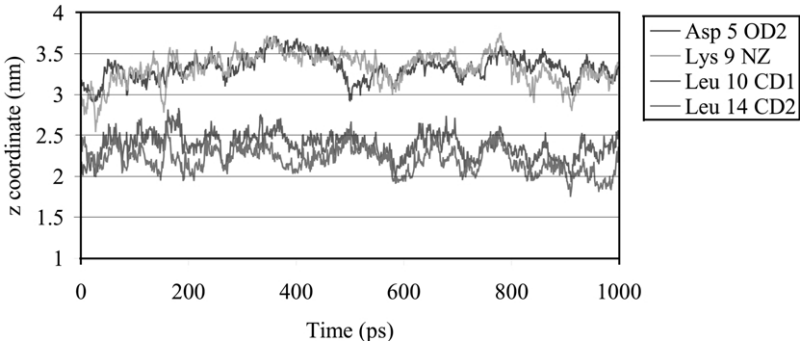

Fig. 6. Time profile of the z coordinate of Asp[5] OD2, Lys[9] NZ, Leu[10] CD1 and Leu[14] CD2 during 1 ns of MD run (simulation 1 in Table 1). The interface between decane and water is 2.7 nm from the bottom of the cell. The starting orientation of the peptide was consistent with NMR data.

map the surface of the peptide in contact with water. This was demonstrated by recording the EPR spectrum of Toac in various conditions. The lineshape did not change with the addition of micelles and was always compatible with the nitroxide being in the fast motion regime (data not shown).

The effect of the spin probes on the peptide resonances was studied by comparing 1D ^{1}H as well as 2D TOCSY spectra in the presence and in the absence of the paramagnetic agents. A comparison between TOCSY spectra obtained with and without the different spin probes is reported in Fig. 1.

In order to quantitatively interpret the results from the NMR experiments, the percentual reduction of the intensity of each HN-Hα cross-peak with and without spin probes was measured. This method has been widely employed [17–21] and provides quick and reliable answers. The advantage of using the reduction of signal intensities instead of the line broadening is the much higher sensitivity and the applicability of the method to partly overlapped peaks with non-symmetric lineshapes [22]. The intensities recorded in the presence of paramagnetic agents were normalized so that the least affected cross-peak has the same intensity with and without the spin probes. The HN-Hβ_1 cross-peak of Asp[5] was chosen for normalization of the TOCSY spectra, in the presence of both 5-DSA and 16-DSA. Normalization eliminates problems arising from a possible reduction in the amount of sample detectable by NMR.

A few peaks in the TOCSY spectra were affected to the same extent by the three spin probes, while most resonances showed very different reduction of intensity, both in the HN-Hα region and in the Hα–Hβ region. In the presence of 5-DSA, remarkable reductions in the intensities of the HN-Hα cross-peaks were observed for most residues (Fig. 2a); this could reflect the very close proximity of the nitroxide to many residues of the peptide. Severe overlap of the cross-peaks of Leu[10] and Leu[14] prevented a reliable measurement of their intensity reduction; the values reported are an average. With the exception of Ile[6] and Leu[7], a rough periodicity in the intensity vs. residue number is apparent. Aside from these two residues, the intensities of five resonances, assigned to the hydrophilic residues Ser[1], Asp[5], Lys[9], Lys[12] and His[16], were reduced less than 30%. These residues are localized on the hydrophilic face of the helix (Fig. 3), and their distance relative to the nitroxide is the largest among all amino acids. All the other residues are localized on the hydrophobic face of the helix, which is larger (over 260°), and undergo larger reductions in the intensity. These results are compatible with the helix being oriented parallel to the micelle surface, since the five residues least affected by 5-DSA are distributed along the entire sequence. The observation that most of the amino acids on the hydrophobic side show large reduc-

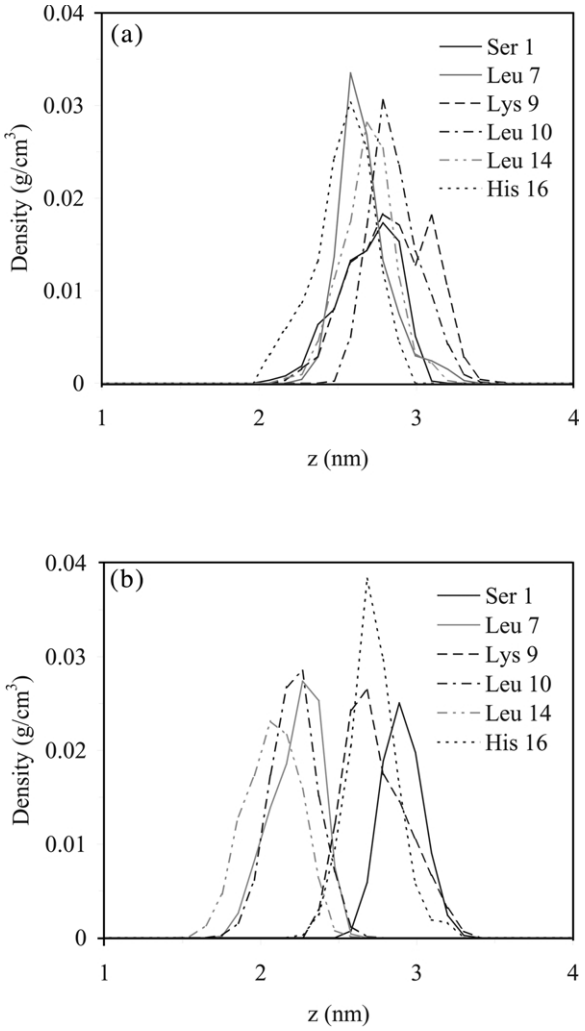

Fig. 7. (a) Density profile of selected amino acids in simulation 6; the helical axis was initially parallel to the interface, with the hydrophobic residues pointing towards the water phase; partial densities were calculated including the side chain atoms and averaged over the initial 200 ps of MD run. (b) Density profiles of the same amino acids, averaged over the last 800 ps of MD run.

tions suggests that the helix is localized close to the micelle surface, and that more than half of the peptide is embedded in the hydrophobic phase.

The effects of 16-DSA are less marked than those of 5-DSA. In the presence of 16-DSA, only four residues undergo a reduction in intensity larger than 30% (Fig. 2b); therefore, the nitroxide of 16-DSA is not in close contact with any residue in the bombolitin. Also, the residues showing the largest reduction in the signal intensity are the same as in the experiments with 5-DSA. Again, this observation is compatible with the peptide being close to the surface rather than embedded in the core of the micelle.

The reduction in signal intensities roughly reproduces the periodicity typical of the α-helix, with Leu^{7}, Leu^{10}, Gly^{11} and Leu^{14} showing the largest reductions. These amino acids are localized on the hydrophobic face of the helix (Fig. 3), together with residues Ile^{3}, Thr^{4}, Ile^{6} and Val^{17}, the resonances of which are reduced by approximately 20%. All the other signals show very small reductions, the lowest ones being observed for Asp^{5} and His^{16}, which are very likely the farthest from the hydrophobic core of the micelle, where the nitroxide is located. Our data show that 16-DSA is more selective than 5-DSA in reducing the NMR signals of bombolitin II, and suggest that the peptide is located at the interface between the micelle and the water phase, with an orientation of the helix axis parallel to the interface.

It has been shown that the broadening of SDS resonances due to the paramagnetic agents is rather selective and clear-cut both for the carbons and the protons [23]. However, our results on the peptide–micelle system show that in a few cases the same residue is strongly affected by both 5-DSA and 16-DSA (e.g. Leu^{10}, Gly^{11} and Leu^{14}), suggesting that the selectivity of the probes may be lower in this case. This effect has been reported before and was tentatively attributed to an increase in the micelle flexibility upon binding to the peptide [23]. Alternatively, fluctuations of the peptide between the micelle surface and the micelle interior could explain this result. The same phenomenon could be responsible for the observation that the periodicity of the nitroxide effect is not very precise. Again, similar results have been reported previously and attributed to rapid averaging in solution [21].

In the series of experiments recorded with Toac at different concentrations it was not possible to compare 2D spectra because of low reproducibility, but careful analysis of 1D spectra provided interesting information for some of the resonances.

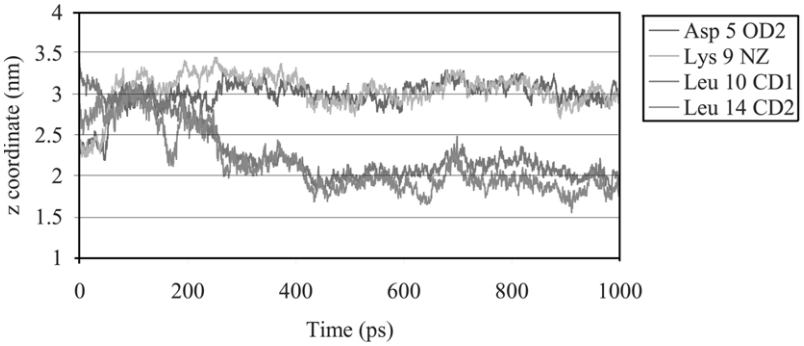

Fig. 8. Time profile of the z coordinate of Asp[5] OD2, Lys[9] NZ, Leu[10] CD1 and Leu[14] CDl during 1 ns of MD run (simulation 6 in Table 1). The interface between decane and water is 2.5 nm from the bottom of the cell. The starting orientation of the peptide was consistent with NMR data.

Since several peaks in the NH region of the 1D spectrum were partially overlapped, spectral deconvolution was necessary to measure accurately the reduction of the intensities. The lineshape chosen for the deconvolution was the sum of a Gaussian and a Lorentzian function, with different weighing coefficients; the frequency of each peak was user defined.

Despite the efforts to improve the analysis, reliable information were obtained only for a few resonances, due to overlap. The linewidth was measured with high accuracy, after deconvolution of the 1D spectra, for the signal of one aromatic proton of His[16], the amide proton of Lys[2] and the C-terminal NH_2. In all these cases, linewidths were more than doubled in the presence of the nitroxide (Fig. 4). Even though it was not possible to measure the line broadening for most signals of hydrophobic residues, it is rather clear from the 1D spectra that the effect of Toac on hydrophilic residues is larger than on the hydrophobic ones (Fig. 4). The reduction of the intensities observed for residues Leu[7], Leu[10], Leu[14] and Gly[11] were much smaller than those observed for aromatic protons of His[16] and for Lys[2]. Moreover, increasing concentrations of Toac caused small paramagnetic shifts for residues Asp[5], His[16] and Thr[4] in particular.

Because of the lack of completeness, these data provide only qualitative information on the exposure of the protons to the solvent. All the residues remarkably influenced by the presence of the water-soluble nitroxide are located on the hydrophilic face of the α-helix, supporting the previous observations and confirming that the orientation of the helical axis is parallel to the micelle surface.

3.2. Molecular dynamics simulations

The structure of bombolitin II in the presence of SDS micelles, as determined by DG–SA calculations, was reported in our earlier work [3]. It consists of an amphipathic helical segment spanning the sequence from residue 2 to residue 16. Here, the same NMR data were used to obtain a starting conformation for further, extensive MD calculations in an anisotropic biphasic cell. One representative lower energy DG structure was chosen as the starting conformation for all the simulations. The conformational features of this structure are consistent with those of the family of structures described previously [3]. The simulations were compared with the results on the orientation of the peptide derived from NMR experiments in the presence of nitroxides.

In the first four restrained MD simulations (Table 1) the starting orientation of the peptide in the simulation box was consistent with the experimental data, i.e. the helical axis was parallel to the water/decane interface and the hydrophilic face was pointing toward water.

Experimentally measured NOEs were imposed as distance restraints to preserve the helical conformation in simulations 1 and 2. As expected, the

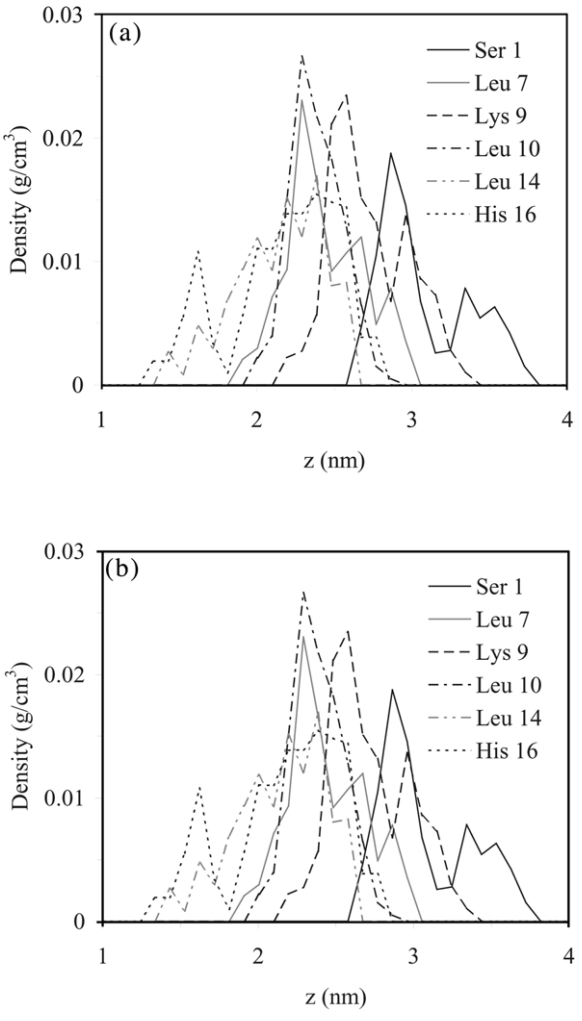

Fig. 9. (a) Density profile of selected amino acids in simulation 10; the helical axis was initially tilted approximately 90° relative to the interface; partial densities were calculated including the side chain atoms and averaged over the initial 200 ps of MD run. (b) Density profiles of the same amino acids, averaged over the last 1000 ps of MD run.

secondary structure of bombolitin II was conserved from residue 2 to residue 15 in both simulations (Table 2). No difference was observed with different electrostatic charges on the peptide. The R.M.S.D. of atomic coordinates and interatomic distances for the backbone atoms was monitored during each simulation, and confirmed that the α-helical secondary structure is very stable. In the third MD run, no distance restraints were used, but still no substantial difference in the secondary structure was observed. To probe the stability of the model, the latter simulation was extended to 10 ns; interestingly, the α-helical conformation was conserved from residue 2 to residue 14 throughout the MD run (Table 2).

In order to get a graphical representation of the average position of the peptide relative to the solvent, the partial density profiles were calculated as a function of the z coordinate for each of the three components of the system (peptide, decane and water) and averaged over the simulation time. Analysis of the partial density profiles in each MD run shows that the distribution of the peptide is broader than the size of the peptide itself (Fig. 5a). If we consider the backbone atoms only, the diameter of a helix is approximately 5 Å; therefore, the helix should span approximately 5 Å in the z direction when its axis is parallel to the interface. Even taking into account slight irregularities in the secondary structure, the density of the backbone atoms should be completely included in approximately 6 or 7 Å in the z direction, while approximately 90% of the partial density is distributed over approximately 12 Å in the first set of simulations. Since the secondary structure is preserved throughout the simulation, our results indicate that the peptide changes its position in the simulation box.

Precise information about the orientation can be obtained from the analysis of the average position of each residue along the z axis. The density profile of each amino acid was calculated including the side chain atoms, and averaged over the simulation time in each of the MD trajectories. In the first set of simulations, approximately 90% of the partial density of the hydrophobic residues is in the range between 1.9 and 3 nm from the bottom of the box, while that of the hydrophilic ones it ranges from 2.5 to 3.7 nm (Fig. 5b). The density profile of each amino acid shows only one maximum, with a relatively narrow distribution, meaning that the orientation of each residue (and of the whole helix) is quite stable on the timescale of 1 ns.

Interestingly enough, no difference was observed between simulations 1 and 2, which

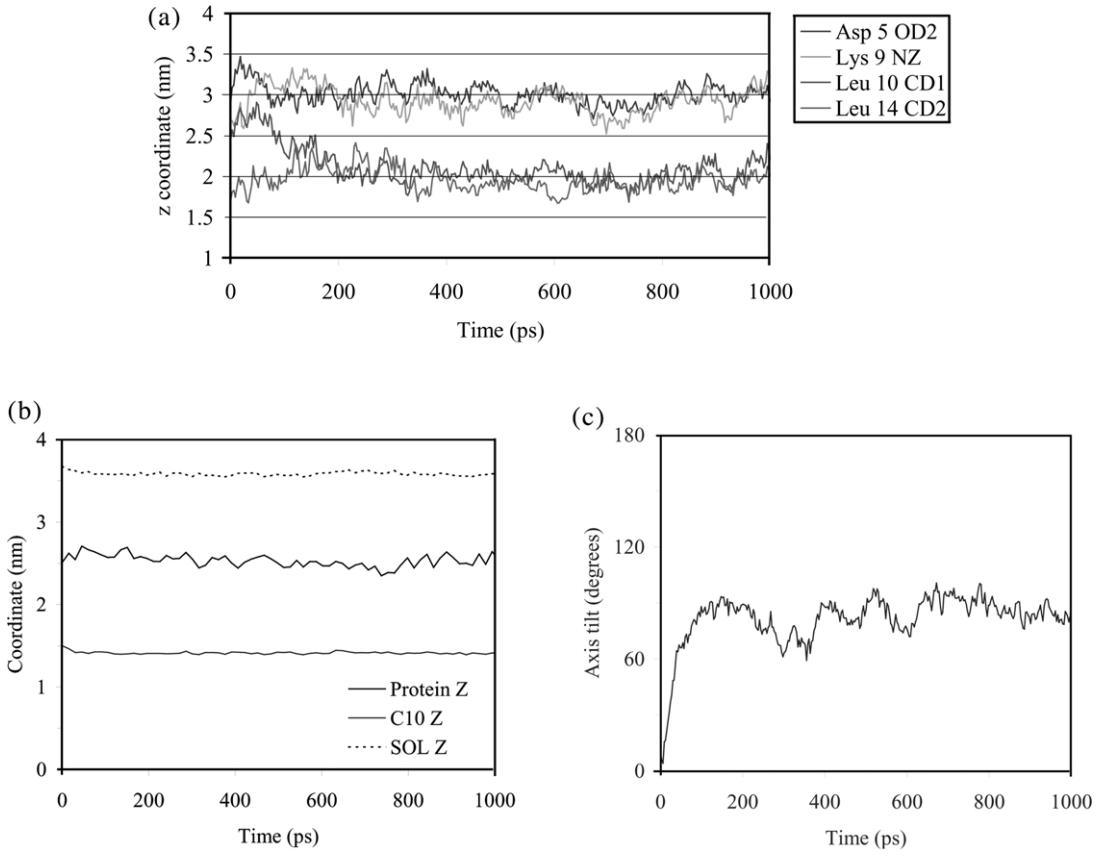

Fig. 10. (a) Time profile of the z coordinate of Asp[5] OD2, Lys[9] NZ, Leu[10] CD1 and Leu[14] CDl during 1 ns of MD run (simulation 10 in Table 1). The interface between decane and water is 2.5 nm from the bottom of the cell. The starting orientation of the peptide was consistent with NMR data. (b) z coordinate of the center of mass of the peptide, water and the decane. (c) Time profile of the tilt angle of the helix.

differ for the electrostatic charges on the side chains (data not shown).

A diagram of the z coordinate of selected atoms as a function of the simulation time provides information on the instant orientation of the peptide relative to the interface, and on the amplitude and the frequency of local motions. The time profile of the z coordinate for side chain atoms of a few selected residues, reported in Fig. 6, shows clearly that no change takes place in the orientation of bombolitin II during the MD simulation up to 10 ns.

In order to challenge the ability of the force field and of the decane/water cell to induce the correct orientation of the peptide even starting from an incorrect one, two sets of MD simulations were performed using initial orientations of the peptide in disagreement with the NMR relaxation data. In simulations 5–7 (Table 1) the helical axis of the peptide was oriented parallel to the interface, but the hydrophilic face was pointed toward decane; in simulations 8–10, the angle between the helical axis and the interface was in the range of 60–90°, and about half of the peptide was embedded in the decane layer. No restraints were applied to maintain or modify the orientation, but the experimentally measured NOEs were imposed as distance restraints to preserve the helical confor-

mation. As shown in Table 2, the secondary structure is α-helical throughout the MD, and is as stable as in the previous cases.

In all these tests the peptide reoriented within 1 ns, and reached a position in agreement with the NMR relaxation data and with the first set of simulations. The plots of the average partial densities vs. the z coordinate show that the distribution of the peptide is slightly broader than in the previous cases, meaning that the peptide undergoes more substantial rearrangements relative to the interface (data not shown). In the second set of simulations, the density profiles of several residues averaged over the initial 200 ps show two maxima, consistent with the existence of two different orientations (Fig. 7). On the contrary, the same density profiles averaged over the last 800 ps of MD run are much narrower and show only one maximum, indicating that the final orientation is stable (Fig. 7). Extending the MD run to 10 ns confirmed the stability of this orientation, which is identical to the experimentally determined one (data not shown).

The timescale for the reorientation was confirmed through the analysis of the time profiles of the z coordinate of selected atoms. The z coordinate was monitored for the same atoms observed in the previous simulations, and the results show clearly that the rotation of bombolitin II about its helical axis takes 100–250 ps in each MD run (see Fig. 8 for simulation 6). It is interesting to observe that, at the same time, slight changes take place in the tilt angle of the helix and in the position of the center of mass; larger deviations from the equilibrium values are observed during the first part of the simulations (data not shown).

As for the third set of simulations (8–10 in Table 1), the density profiles are the broadest and for most residues show two maxima when averaged over the first part of the MD, but only one maximum when averaging is over the last part (Fig. 9a and b). The major changes in the peptide orientation that take place during the first 150–450 ps of MD run involve significant variations of the partition of the bombolitin between the solvent phases. In all cases, the final orientation is identical to the experimentally determined one. Extending the simulation time to 10 ns does not cause any further change in the orientation of the peptide; the fluctuations of the peptide on the interface in the last 9 ns of simulations 7 and 10 have the same amplitude as those observed in simulations 1–3. Also in this case, the plot of the time profile of the z coordinate of selected atoms provides the most reliable information on the timescale of the motion (Fig. 10a). The rearrangements involve the modification of the tilt angle, the displacement in the center of mass of the peptide (Fig. 10b and c) and the rotation about the helical axis. Obviously, the main contribution to the reorientation comes from the change in the angle between the helical axis and the z axis, which changes from a value of approximately 0° (at the beginning of simulation 10) to the equilibrium value of 90° within the first 100–200 ps (as shown in Fig. 10c).

Assuming that the interface is the region where decane and water partial densities are nearly identical, its average position can be determined during an MD run. For example, in simulation 1 the interface is found at 2.7 nm from the bottom of the box (Fig. 5a). In all the MD runs, the peptide is very close to the interface, in the region where the partial densities of decane and water drop to zero (Table 2and Fig. 5a). These results are typical for a surface-bound peptide; however, the center of mass of the peptide is generally found slightly shifted toward the water phase. This is one of the differences between the results of the simulations and those of the NMR relaxation experiments, and it is probably due to the inaccuracy of the description of the interface in the MD simulation. In fact, a strong interaction with the surface of SDS micelles is a very common feature for basic amphipathic peptides [24,25] and is a consequence of the electrostatic interaction between the positively charged side chains of lysines, arginines and histidines and the negatively charged headgroups of the SDS micelle. Such interactions cannot be reproduced by the decane layer.

4. Conclusions

In the present study, the orientation of bombolitin II was analyzed in the presence of a

membrane-mimicking environment, provided by SDS micelles.

NMR experiments were carried out using 5-DSA, 16-DSA and Toac as spin probes to induce selective effects on the NMR resonances of the peptide according to the position of the nitroxide group relative to the micelle.

It is well known that the nitroxide group of 5-DSA is located close to the sulfate group of the SDS; in this study we showed that the nitroxide has lower effects on the protons exposed to the solvent, i.e., those of Asp^5 and His^{16}. The reduction in intensity caused by the doxyl group of 16-DSA, localized in the micelle core, was in general less marked than that induced by 5-DSA and almost negligible for most protons on the hydrophilic face of the helix.

In all measurements, both with 5-DSA and 16-DSA, a modulation of the effect was observed with the approximate periodicity of the α-helix, in line with previous results [3].

Furthermore, the reduction in intensity of specific proton signals indicates that the peptide is located on the surface of the micelle, with its helical axis parallel to the interface. The orientation experimentally determined is in good agreement with the predictions based on the Eisenberg model.

The results obtained with 16-DSA suggest that only a small part of the helix surface is exposed to water, while the rest of the peptide is embedded in the micelle, and particularly residues Ile^3, Leu^7, Gly^{11}, Leu^{10} and Leu^{14}. This deep embedding is due to the very narrow hydrophilic surface of bombolitin II ($<100°$). This particular feature may allow the peptide to alter the aggregation state of the phospholipid membrane, which in turn is supposed to be responsible for the activation of PLA_2.

The MD is able to simulate the behavior of the peptide. The starting orientation of the peptide at the water/decane interface is not critical, since the peptide reorients within a few hundreds of picoseconds. The simple rotation of the peptide about its helical axis takes approximately 100–200 ps in each MD run, while the alignment of the helical axis with the interface takes from 150 to 450 ps depending on the initial orientation.

The decane/water system is able to reproduce the main features of the peptide/micelle interaction. The imprecise definition of the polar interface is most likely responsible for the differences between the experiments and the simulations.

References

[1] A. Argiolas, J. Pisano, Bombolitins, a new class of mast cell degranulating peptides from the venom of the bumblebee *Megabombus pennsylvanicus*, J. Biol. Chem. 260 (1985) 1437–1444.

[2] E. Bairaktari, D.F. Mierke, S. Mammi, E. Peggion, Conformations of bombolitins I and III in aqueous solutions: circular dichroism, ^{1}H NMR, and computer simulation studies, Biochemistry 29 (1990) 10097–10102.

[3] R. Battistutta, A. Pastore, S. Mammi, E. Peggion, Conformational properties of the amphipathic lytic polypeptide bombolitin II. A circular dichroism, NMR and computer simulation study, Macromol. Chem. Phys. 196 (1995) 2827–2841.

[4] D. Eisenberg, R. Weiss, T. Terwilliger, The helical hydrophobic moment: a measure of the amphiphilicity of a helix, Nature 299 (1982) 371–374.

[5] J. Segrest, H. De Loof, J. Dohlman, C. Brouillette, G. Anantharamaiah, Amphipathic helix motif: classes and properties, Proteins 8 (1990) 103–117.

[6] G. Signor, S. Mammi, E. Peggion, H. Ringsdorf, A. Wagenknecht, Interaction of bombolitin III with phospholipid monolayers and liposomes and effect on the activity of phospholipase A_2, Biochemistry 33 (1994) 6659–6670.

[7] B.L. Bales, L. Messina, A. Vidal, M. Peric, O.N. Nascimento, Precision relative aggregation number determinations of SDS micelles using a spin probe. A model of micelle surface hydration, J. Phys. Chem. B 102 (1998) 10347–10358.

[8] C. Griesinger, G. Otting, K. Wüthrich, R.R. Ernst, Clean TOCSY for ^{1}H spin system identification in macromolecules, J. Am. Chem. Soc. 110 (1988) 7870–7872.

[9] M. Piotto, V. Saudek, V. Sklenar, Gradient-tailored excitation for single-quantum NMR spectroscopy of aqueous solutions, J. Biomol. NMR 2 (1992) 661–665.

[10] H.J.C. Berendsen, D. van der Spoel, R. van Drunen, GROMACS: a message-passing parallel molecular dynamics implementation, Comp. Phys. Comm. 91 (1995) 43–56.

[11] H.J.C. Berendsen, J.P.M. Postma, W.F. van Gunsteren, J. Hermans, Intermolecular Forces, D. Reidel Publishing Company, Dordrecht, 1981, pp. 331–342.

[12] H.J.C. Berendsen, J.P.M. Postma, W.F. van Gunsteren, A. Di Nola, J.R. Haak, Molecular dynamics with cou-

pling to an external bath, J. Chem. Phys. 81 (1984) 3684–3690.
[13] D.P. Tieleman, H.C.J. Berendsen, M.S.P. Sansom, Voltage-dependent insertion of a channel forming peptide: molecular dynamics simulations of alamethicin at phospholipid/water and octane/water interfaces, Biophys. J. 80 (2001) 331–346.
[14] K.A. Feenstra, B. Hess, H.J.C. Berendsen, Improving efficiency of large time-scale molecular dynamics simulations of hydrogen-rich systems, J. Comp. Chem. 20 (1999) 786–798.
[15] B. Hess, H. Bekker, H.J.C. Berendsen, J.G.E.M. Fraaije, LINCS: a linear constraint solver for molecular simulations, J. Comp. Chem. 18 (1997) 1463–1472.
[16] W. Kabsch, C. Sander, Dictionary of protein secondary structure: pattern recognition of hydrogen-bonded and geometrical features, Biopolymers 22 (1983) 2577–2637.
[17] H.W. Van Den Hooven, C.A.E.M. Sponk, M. Van De Kamp, R.N.H. Konings, C.W. Hilbers, F.J.M. Van De Ven, Surface location and orientation of the lantibiotic nisin bound to membrane mimicking micelles of dodecylphosphocholine and sodium dodecylsulphate, Eur. J. Biochem. 235 (1996) 394–403.
[18] V. Chapin, J. Leenhouts, A. de Kroon, B. de Kruijff, Secondary structure and topology of a mitochondrial presequence peptide associated with negatively charged micelles. A 2D ^{1}H-NMR study, Biochemistry 35 (1996) 3141–3146.
[19] M. Pellegrini, M. Royo, M. Chorev, D.F. Mierke, Conformational characterization of a peptide mimetic of the third cytoplasmic loop of the G-protein coupled parathyroid hormone/parathyroid hormone related protein receptor, Biopolymers 40 (1996) 653–666.
[20] M. Pellegrini, A. Bisello, M. Rosenblatt, M. Chorev, D.F. Mierke, Binding domain of human parathyroid hormone receptor: from conformation to function, Biochemistry 37 (1998) 12737–12743.
[21] A. Piserchio, A. Bisello, M. Rosenblatt, M. Chorev, D.F. Mierke, Characterization of parathyroid hormone/receptor interactions: structure of the first extracellular loop, Biochemistry 39 (2000) 8153–8160.
[22] M. Lindberg, A. Gräslund, The position of the cell penetrating peptide penetratin in SDS micelles determined by NMR, FEBS Lett. 497 (2001) 39–44.
[23] M. Lindberg, J. Jarvet, Ü. Langel, A. Gräslund, Secondary structure and position of the cell penetrating peptide Transportan in SDS micelles as determined by NMR, Biochemistry 40 (2001) 3141–3149.
[24] P. La Rocca, P.C. Biggin, D.P. Tieleman, M.S.P. Sansom, Simulation studies of the interaction of antimicrobial peptides and lipid bilayers, Biochim. Biophys. Acta 1462 (1999) 185–200.
[25] T. Wymore, T.C. Wong, Molecular dynamics study of substance P peptides partitioned in a sodium dodecylsulfate micelle, Biophys. J. 76 (1999) 1213–1227.